Odd−Even Effect of Flexible Spacer Length on Flow-Induced Isotropic-to-Nematic Transition in Segmented Thermotropic Polymers

Patrick T. Mather*,† and Hong G. Jeon‡

Polymer Program and Chemical Engineering Department, University of Connecticut, Storrs, Connecticut 06269, and Systran Corp., AFRL/MLBP, 2941 P Street Suite 1, Wright Patterson AFB, Ohio 45433-7750

Chang Dae Han* and Sukky Chang

Department of Polymer Engineering, The University of Akron, Akron, Ohio 44325-0301

Received September 4, 2001; Revised Manuscript Received November 13, 2001

ABSTRACT: The dependence of the flow-induced isotropic-to-nematic (I−N) phase transition phenomenon on the spacer length is investigated using the well-behaved thermotropic polymers, PSHQ*n*, with *n* representing the number of methylene groups as flexible spacer in the main chain. Using optical microrheology methods and mechanical rheological methods, the critical shear rate ($\dot{\gamma}_{cr}$) required for the onset of nematic-phase formation is measured at temperatures above the quiescent I−N transition temperature (T^{o}_{IN}). In particular, flow-induced birefringence is measured for the PSHQ*n* polymers of varying spacer lengths as functions of both temperature and shear rate. As shear rate increases for a fixed temperature higher than the T^{o}_{IN}, a clear transition from low-level birefringence (0.0−0.005) to nematic-level birefringence (>0.01) is observed for most PSHQ*n* polymers. Interestingly, the $\dot{\gamma}_{cr}$ for nematic-phase formation is significantly larger for even-numbered PSHQ*n* compared to odd-numbered PSHQ*n*. This odd−even effect is explained by a significant difference in steady shear viscosity (and terminal relaxation time) at fixed temperature above T^{o}_{IN}. A critical dimensionless group, critical Deborah number $De_{cr} = \dot{\gamma}_{cr}\tau$ with τ being the terminal relaxation time of polymer, is introduced to explain the experimental observations.

Introduction

Research into the response of thermotropic liquid-crystalline polymers (TLCPs) to shear flow has the ultimate goal of both understanding the complex coupling between kinematics and orientational order and subsequently applying this knowledge to the design of processes which yield superior articles from this class of materials. Today it is well established that the rheological behavior and the time evolution of the structure of TLCPs depend on thermal and deformation histories.[1−3] Therefore, such investigations requires well-characterized *model* polymers that can give rise to reproducible rheological responses to shear flow.

Earlier, Han and co-workers[4−7] investigated shear startup, intermittent shear flow, and stress relaxation upon cessation of shear flow of the semiflexible main-chain TLCPs, poly[(phenylsulfonyl)-*p*-phenylene alkylenebis(4-oxybenzoate)s] (PSHQ*n*), with chemical structure

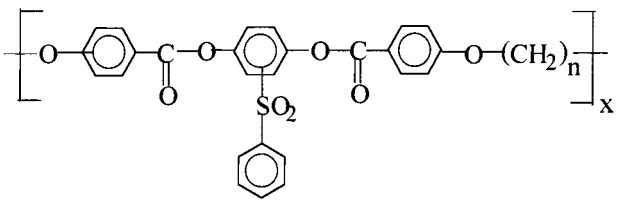

with varying numbers (n = 3−12) of methylene groups as flexible spacers. It was identified that imposition of a steady shear flow of a sufficient magnitude *in the isotropic phase* could lead to dramatic shear thinning with long duration changes and structural recovery over a time scale proportional to the time and magnitude of previous shearing. They have pursued the rheological characterization of the well-characterized PSHQ*n* featuring "monoflexibility" along with accessible and narrow nematic-to-isotropic (N−I) transition temperature (T_{NI}). The study of such TLCPs has allowed for the successful determination of such structure−property relations as the influence of spacer length on shear startup dynamics, etc.[8] Additionally, the use of such polymers provides an alternative to studying the rheological properties of commercial copolyester systems (e.g., Vectra polymer series) that have difficulties with erasing previous thermal and deformation histories, owing to the lack of an accessible clearing temperature, and thus with obtaining a reproducible initial condition.

Using rheo-optical methods, Mather et al.[9] have shown direct evidence that a flow-induced isotropic-to-nematic (I−N) transition occurs in PSHQ10 at temperatures near the quiescent I−N transition temperature (T^{o}_{IN}). They have shown further, direct microscopic evidence of the nucleation of nematic phase in shear flow for the same polymer. In that study, they observed that shear flow of PSHQ10 above the clearing temperature (T_{NI} = 177 °C) led to the nucleation of highly birefringent nematic threads in the polymer and that the fraction of nematic increased with increasing shearing strain. Upon removal of shear flow, the nematic ordering that had formed relaxed over a time scale comparable to that observed for the recovery of linear viscoelastic properties. Furthermore, examination of the light intensity transmitted between crossed polarizers under conditions of increasing shear rate and increasing

† University of Connecticut.
‡ Systran Corp.

10.1021/ma0115601 CCC: $22.00
Published on Web 01/18/2002

temperature enabled the establishment of a nonequilibrium phase diagram.

A recent report of the flow-induced nematic phase in a side-chain liquid crystalline polymer (SCLCP)[10] has shown that in such systems—phenyl benzoate mesogens attached through a flexible linkage to a methacrylate backbone—substantial positive birefringence indicative of a nematic phase appears above a critical shear rate ($\dot{\gamma}_{cr}$). Above a second $\dot{\gamma}_{cr}$, conversion to nematic phase is apparently completed as evidenced by saturation in birefringence, with respect to shear rate ($\dot{\gamma}$), at levels of 0.001−0.003. Attributed to independence of mesogen dynamics from backbone dynamics afforded by the hexamethylene spacer employed, the authors reported quite high $\dot{\gamma}_{cr}$ values, ranging from 5 to 35 s^{-1}, when compared to previous data on the main-chain TLCP, PSHQ10.[9] Nonetheless, it was pointed out that a 1000-fold disparity existed between the characteristic shear time ($1/\dot{\gamma} \sim 0.01$ s) and the shorter time characteristic of mesogen relaxation, suggesting that a "network structure" with longer relaxation time must exist. Importantly, the reported shear stress measurements with increasing $\dot{\gamma}$ revealed a plateau stress that exists for intermediate shear rates where isotropic and nascent nematic phases coexist; i.e., nematic conversion is incomplete. This plateau appears to be a salient feature of flow-induced nematicity that, for lyotropic solutions of rigid rods, has been explained in terms of "shear band" formation with the existence of N−I interface preserving the state of constant stress (on increasing $\dot{\gamma}$) until full conversion has occurred.[11]

I−N transitions in shear flow have been reported in another distinct system, namely, concentrated wormlike micelles.[12] In this case, the materials consist of multiple components (cetylpyridinium chloride/hexanol/salt-water) and complex phase behavior, including isotropic wormlike micelles at low concentrations, nematic wormlike micelles at intermediate concentrations, and hexagonal packing at high concentrations. On shearing solutions of nematic wormlike micelles, shear stress measurements revealed a stress plateau that coincided with the critical onset of long-range orientation evidenced by cresent formation in small-angle neutron scattering observations.

While studies of the I−N transition in flow have revealed features common to multiple systems, many questions remain, particularly concerning molecular details of the transition. The present study was motivated by the desire to understand the odd−even effect of flexible spacer length in controlling the nature of the flow-induced I−N transition. To do this, we have adopted an experimental approach that involved quantitative in-situ measurements of orientational ordering above the quiescent transition temperatures of a homologous series of PSHQ*n* polymers. This paper presents the highlights of our findings.

Experimental Section

Materials. The polymers, PSHQ*n* with *n* ranging from 6 to 10, used in the present study were synthesized in a previous study of Chang and Han.[13] The details of the polymer synthesis are described in the literature,[14,15] and the thermal transition temperatures of PSHQ*n* are given in a previous paper.[13] Thermogravimetric measurements have shown that PSHQ*n* polymers degrade at temperatures above 350 °C, well above their T_{NI}.

Sample Preparation. Specimens for rheo-optical and rheological characterization were prepared by first dissolving PSHQ*n* ($n = 7-10$) in dichloromethane in the presence of 0.1 wt % antioxidant (Irganox 1010, Ciba-Geigy Group) and then slowly evaporating the solvent at room temperature for 1 week. However, specimens of PSHQ6 were cast from 1,1,2,2-tetrachloroethane (also in the presence of 0.1 wt % antioxidant), because this polymer does not dissolve in dichloromethane. The cast films (1 mm thick) were further dried in a vacuum oven at room temperature for at least 3 weeks and, prior to measurements, at 90 °C for 48 h in order to remove any residual solvent and moisture.

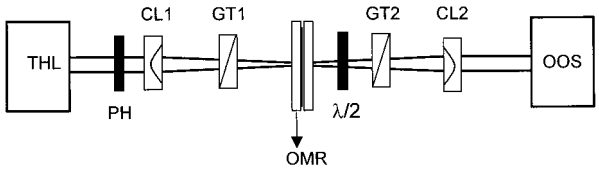

Figure 1. Schematic representation of the optical train employed to measure birefringence during shear flow at elevated temperatures. Light from a lamp (THL) passes through a pinhole (PH), condensing lens (CL1), Glan-Thompson polarizer (GT1), and then through a heater slot in the custom planar Couette flow device (OMR). Emerging light then passes through a multiorder $\lambda/2$ plate and through a second polarizer (GT2) and collected with a condensing lens (CL2) to a visible spectrometer (OOS) along fiber-optic cable for analysis.

Rheo-Optics. To quantify flow-induced ordering through the I−N transition in shear flow, we have employed a custom-built optical microrheometer described in some detail previously.[8,9,16] Two experimental configurations were used in particular: one with the rheometer mounted within a polarizing optical microscope (POM) and the other with the rheometer mounted within a modified spectrographic birefringence optical train, shown in Figure 1 and described further below. In both cases, the microrheometer employed consists of parallel quartz plates held 50.8 μm apart, heated with independent temperature controllers, and with one plate assembly translating at a controlled velocity relative to the other fixed plate using a microstepping motor and customized linear translation stage. In contrast to other designs,[10] the apparatus has a long travel that enable shear strains as larger than 100 strain units for samples 50 μm thick. Interested readers are directed to our previous publications.[8,9,16]

Polarizing optical microscopy images were collected in-situ using the microrheometer mounted on an aus Jena polarizing microscope equipped with a 25× objective lens and a Panasonic KR222 CCD camera (793 × 493 pixels). Crossed polarizers were arranged with the polarizer oriented along the horizontal flow axis (H_V POM configuration).

To measure birefringence, we have used the optical method of spectrographic birefringence adapted in our laboratory for application to heated polymers undergoing controlled shear. Referring to Figure 1, white light from a tungsten halogen lamp (THL) passes through a fiber-optic cable to an assembly consisting of a pinhole (PH), condensing lens (CL1), and Glan-Thompson polarizer (GT1) and then through a heater slot in the microrheometer heater slot (OMR).[17] The emerging light passes through a second polarizer (GT2) oriented parallel with the first and then collected with a condensing lens (CL2)/fiber-optic assembly to a visible spectrometer (OOS, Ocean Optics S2000) for quantitative analysis. For the present study, the sensitivity of this optical arrangement applied to low shear rates is inadequate for measuring low birefringence levels. Thus, we have modified the optical train used in prior investigations[8,16] to include a static retardation plate (multiorder $\lambda/2$ plate, Figure 1), after the sample and before the second polarizer, oriented along the flow axis and at an angle of $\pi/4$ with the parallel polarizer/analyzer. This arrangement yields multiple oscillations in the absence of sample birefringence. In the presence of flow, the oscillations (interference fringes) translate to the left for positive birefringence and to the right for negative birefringence, assuming orientation along the flow axis. Thus, application of our fast Fourier

transform (FFT) analysis method to the reference spectra (no shear) and then to samples of unknown birefringence allows the extraction of samples retardance, D_{sample} (and thus birefringence), by simple subtraction of the reference retardance (D_{mo}) from the total retardance (D_{tot}); i.e., $D_{tot} = D_{mo} + D_{sample}$, where D is the retardance gleaned from spectral analysis. In particular, with the parallel polarizers and waveplate arranged as described, the transmission spectrum follows:

$$T(\lambda) = A_S \cos^2\left(\pi \frac{D_{mo} + \Delta n h}{\lambda}\right) \tag{1a}$$

where A_S is the spectrum amplitude, D_{mo} is the static retardance of the multiorder waveplate (ca. 20 μm), Δn is the birefringence projected on the velocity−vorticity plane, h is the specimen thickness, and λ is the applied wavelength. Also, $T(\lambda)$ is the normalized spectrum,

$$T(\lambda) = (I(\lambda) - I_d(\lambda))/(I_0(\lambda) - I_d(\lambda)) \tag{1b}$$

with $I_0(\lambda)$ being the transmitted spectrum of the isotropic polymer at rest, $I_d(\lambda)$ the dark spectrum observed with the detection optics blocked, and $I(\lambda)$ the measured spectrum during flow. Thus, in the absence of sample birefringence ($\Delta n = 0$), interference fringes are observed; addition of a small level of sample birefringence along the flow axis will decrease the fringe spacing or increase the FFT frequency.[8] With this method, we can measure sample retardances from zero to approximately 50 μm with high resolution. We note that the birefringence measured is Δn_{13} (=D/h) where the subscripts 1 and 3 refer to the velocity and vorticity axes, respectively. To minimize effects of dispersion in both n_e, the slow-axis refractive index, and n_0, the fast axis refractive index, we have limited the spectrum breadth to the range $550 < \lambda < 750$ nm.

Data Analysis. To determine the $\dot{\gamma}_{cr}$ for nematic phase formation, we have adopted a data fitting scheme (for $\Delta n - \dot{\gamma}$ data) that is robust and also accounts for all of the data collected. In particular, data fitting was performed by fitting with a three-parameter logistics function,

$$\Delta n = \frac{\Delta n_\infty}{1 + (\dot{\gamma}_0/\dot{\gamma})^\beta} \tag{2}$$

Furthermore, the reported shear rate threshold for nematic-phase formation was chosen as the shear rate where 5% of the full (nematic) birefringence has been achieved. The choice in threshold was found to yield very reproducible assessment of critical shear rate; lower values approached our sensitivity limit while higher values were never reached for some conditions. More details concerning this use of eq 2 in fitting experimental data will be presented in the results section below.

Rheological Measurement. A Rheometrics mechanical spectrometer (RMS model 800) in the parallel-plate configuration (8 mm diameter plates) was used to measure the dynamic storage and loss moduli, $G'(\omega)$ and $G''(\omega)$, as functions of angular frequency (ω) at temperatures above the T_{NI} of each polymer. The strain amplitude was varied from 0.01 to 0.06, which was well within the linear viscoelastic regime of the PSHQ*n* polymers investigated. Also, the cone-and-plate configuration (8 mm diameter plate and 4° cone angle) was used to run steady-state shear flow as functions of shear rate ($\dot{\gamma}$) at temperatures above the T_{NI} of each polymer. Data acquisition was accomplished with a microcomputer interfaced to the rheometer. All experiments were conducted under a nitrogen atmosphere to prevent oxidative degradation. The temperature control was accurate to within ±1 °C.

Results and Discussion

Thermal Transitions. As previously reported,[13] PSHQ*n* polymers display an odd−even fluctuation in both the nematic−isotropic and glass transition temperatures, the latter fluctuation being smaller in magnitude. As the N−I (or "clearing") transition is first-order in nature, featuring significant supercooling, the values of T_{IN} in the limit of zero cooling rate (T^o_{IN}) are the reference transition temperatures for flow-induced transition measurements. Thus, Figure 2 reports the T_{IN} data obtained by extrapolating cooling DSC data to zero cooling rate and T_g data as functions of the number (n) of methylene groups. It is seen that the transition temperatures of PSHQ*n* polymers with odd-numbered n and even-numbered n decrease with increasing n, but with fluctuations where PSHQ*n* polymers with even-numbered n have higher transition temperatures. For our flow-induced transition experiments, the spacer length comparisons are made at fixed ΔT values, where $\Delta T = T - T^o_{IN}$. We note, however, that because the magnitude of T_g fluctuation is relatively small, viscosity differences arising from different $\Delta T' = T - T_g$ (i.e., free volume differences) are unavoidable. In fact, values of $T_{IN} - T_g$ (from Figure 2) show the magnitude of this effect also with significant odd−even fluctuation: 110, 76, 88, 75, and 80 °C for PSHQ6 through PSHQ10, respectively.

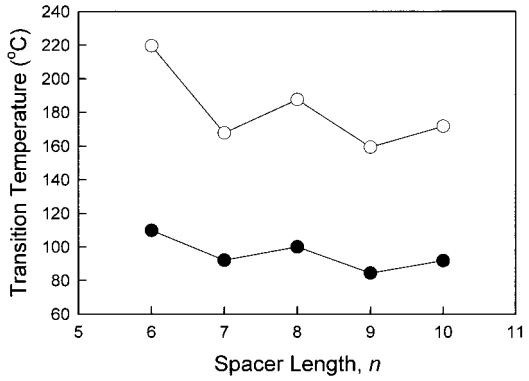

Figure 2. Plot of isotropic−nematic transition temperature (T^o_{IN}), open symbols, and glass transition temperature (T_g), closed symbols, vs spacer length.[13] T^o_{IN} data are obtained by extrapolating peak exotherm temperatures observed with differential scanning calorimetry (DSC) for varying cooling rate while T_g data are obtained during DSC heating runs at 20 °C/min.

Earlier, Chang and Han[13] speculated that the chains of PSHQ*n* polymers with even-numbered n would have an alignment of rigid cores along one preferred symmetry axis giving rise to well-packed (*crystallizable*) nematic phase, while the chains of PSHQ*n* polymers with odd-numbered n would possess configurational restrictions imposed by intramolecular correlations and thus feature frustrated alignment of rigid cores along one preferred symmetry axis. The latter gives rise to a poorly packed (*glass-forming*) nematic phase. In other words, the differences in chain conformation between PSHQ*n* polymers with even-numbered n and PSHQ*n* polymers with odd-numbered n are believed to be responsible for the observed odd−even effect in T_{NI}.

Rheological Properties in the Isotropic Phase. To address differences in viscosity due to both $\Delta T'$ and molecular weight variations between samples, we have determined the terminal relaxation time (τ) using linear viscoelastic data as functions of temperature. In the present study, τ for each polymer in the isotropic phase is calculated using the relationship $\tau = \eta_0 J^o_e$, where η_0 is zero-shear viscosity and J^o_e is steady-state compliance. η_0 and J^o_e, respectively, are calculated from $\eta_0 = \lim_{\omega\to 0}[G''(\omega)/\omega]$ and $J^o_e = \lim_{\omega\to 0}\{G'(\omega)/[G''(\omega)]^2\}$ using

Table 1. Relaxation Time (τ) of PSHQ*n* Investigated in This Study

(a) PSHQ6 (T_{NI} = 228 °C)

T (°C)	$\eta_0 \times 10^{-3}$ (Pa s)	$J_e^o \times 10^5$ (Pa^{-1})	τ(s) $\times 10^2$ (s)
235	3.600	0.971	3.494
240	2.887	1.123	3.243
245	2.353	1.312	3.086
250	1.839	1.347	2.477

(b) PSHQ7 (T_{NI} = 171 °C)

T (°C)	$\eta_0 \times 10^{-5}$ (Pa s)	$J_e^o \times 10^5$ (Pa^{-1})	τ (s)
180	1.949	2.652	5.168
185	1.373	3.663	5.030
190	0.915	5.100	4.666
195	0.547	5.719	3.131

(c) PSHQ8 (T_{NI} = 199 °C)

T (°C)	$\eta_0 \times 10^{-3}$ (Pa s)	$J_e^o \times 10^6$ (Pa^{-1})	τ (s) $\times 10^2$ (s)
205	0.907	6.957	0.631
210	0.659	6.413	0.423
215	0.492	6.635	0.327
220	0.406	6.684	0.272

(d) PSHQ9 (T_{NI} = 162 °C)

T (°C)	$\eta_0 \times 10^{-5}$ (Pa s)	$J_e^o \times 10^5$ (Pa^{-1})	τ (s)
170	1.665	1.324	2.205
175	1.179	1.413	1.656
180	0.921	1.035	0.957

(e) PSHQ10 (T_{NI} = 177 °C)

T (°C)	$\eta_0 \times 10^{-4}$ (Pa s)	$J_e^o \times 10^5$ (Pa^{-1})	τ (s)
180	1.520	2.466	0.375
185	1.200	2.103	0.252
190	0.885	2.086	0.185
191	0.794	2.128	0.169
192	0.720	2.083	0.150
193	0.634	2.096	0.133
196	0.451	1.747	0.078

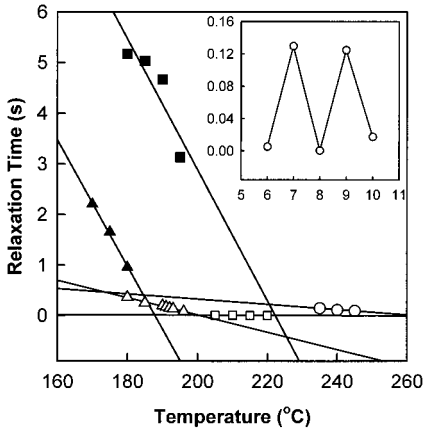

Figure 3. Mechanical relaxation time ($\tau = \eta_0 J_e^o$) for PSHQ6 (○), PSHQ7 (■), PSHQ8 (□), PSHQ9 (▲), and PSHQ10 (△) as functions of temperature. Straight lines are from linear regression fits. Inset shows the slope of these lines as a function of spacer length with units of s/°C for the slope.

oscillatory shear data. Numerical values of η_o, J_e^o, and τ for the PSHQ*n* polymers investigated in this study are summarized in Table 1. The results of such testing are shown in Figure 3, where we see two major distinctions between even-numbered and odd-numbered PSHQ*n*. First, values of the relaxation time, τ, for PSHQ7 and PSHQ9 are large, ranging from 1 to 6 s, compared to PSHQ6, PSHQ8, and PSHQ10, with $2 \times 10^{-3} < \tau < 0.4$ s. Second, the magnitude of the negative slope in τ vs T plots is substantially higher for odd-numbered PSHQ*n* as shown in the inset figure. These τ data will be used later when considering the critical shear rate magnitude, $\dot{\gamma}_{cr}$, for I−N transition in polymers of vastly different relaxation times. Further, we also measured steady-state shear flow properties of each polymer in the isotropic phase using a cone-and-plate rheometer. Such experimental results are necessary to help interpret the results of our rheo-optical study that are presented below.

POM Observations of Flow-Induced I−N Transition. The nature of the flow-induced I−N transition is most readily observed through direct visualization with polarizing optical microscopy (POM). Figure 4 shows a sequence of in-situ POM images for PSHQ7 (a typical odd-numbered PSHQ*n*), during shear startup at T = 177 °C (ΔT = 9 °C) and $\dot{\gamma}$ = 0.251 s^{-1}, a shearing experiment above the $\dot{\gamma}_{cr}$ for nematic-phase formation, and using crossed polarizers with the polarizers aligned along the flow axis. For this temperature, flows with $\dot{\gamma} < 0.05$ s^{-1} resulted in no detectable birefringence. Inspection of Figure 4 reveals quite uniform birefringence, apparently devoid of both droplet/matrix interfaces and disclination texture, at least at our relatively low magnification. In addition to the observed uniformity, POM reveals two notable features. First, weak striations of width 5−10 μm appear along the flow direction. The striations are most apparent at t = 10 s and t = 40 s, where the total transmitted intensity is moderate. Second, it is clear that the transmitted intensity in this crossed polarizer arrangement goes through a maximum near t = 30 s or $\dot{\gamma}t$ = 7.5. This is an indication of substantial orientation away from the flow axis during startup that yields to flow alignment parallel to the flow axis after more shear strain has accumulated (t = 160 s). Although no domains are clearly visible for the micrograph at t = 30 s, we postulate that numerous microdomains exist, with size below our detectable limit and with a distribution of orientations biased away from the flow axis but with uniformly high internal orientation.

In contrast to odd-numbered PSHQ*n* polymers, even-numbered PSHQ*n* polymers require about a 10-fold higher $\dot{\gamma}$ for I−N transition and yield distinct textures indicative of nematic fibrils in an isotropic matrix. As a typical example, Figure 5 displays a sequence of POM images during shear startup at T = 232 °C (ΔT = 12 °C) and $\dot{\gamma}$ = 3.98 s^{-1} for PSHQ6. Shortly after flow inception (4 s), the sample adopts a bright pale blue and homogeneous appearance that, upon further shearing, transforms to one of significant heterogeneity with coarse striations along the flow axis (~25 μm) and fine fibrils of 5 μm diameter oriented in a criss-cross pattern biased toward angles ±45° with respect to the flow axis. As highlighted in our recent paper on rheo-optics of PSHQ*n* blends,[18] such a bias is a reflection of the use of crossed polarizer optics where sensitivity to fiber orientations, $\chi = n\pi/4$ (n = 1, 2), is greatest. Thus, although we are unable to ascertain with the present data the distribution of nematic fibril orientations, it is clear that a significant population with orientations away from the flow axis exists. Beyond t = 8 s, the texture has reached a steady state. We will show below that the observed textural evolution behavior for PSHQ*n* polymers occurs with overall birefringence levels in the range consistent with a nematic phase.

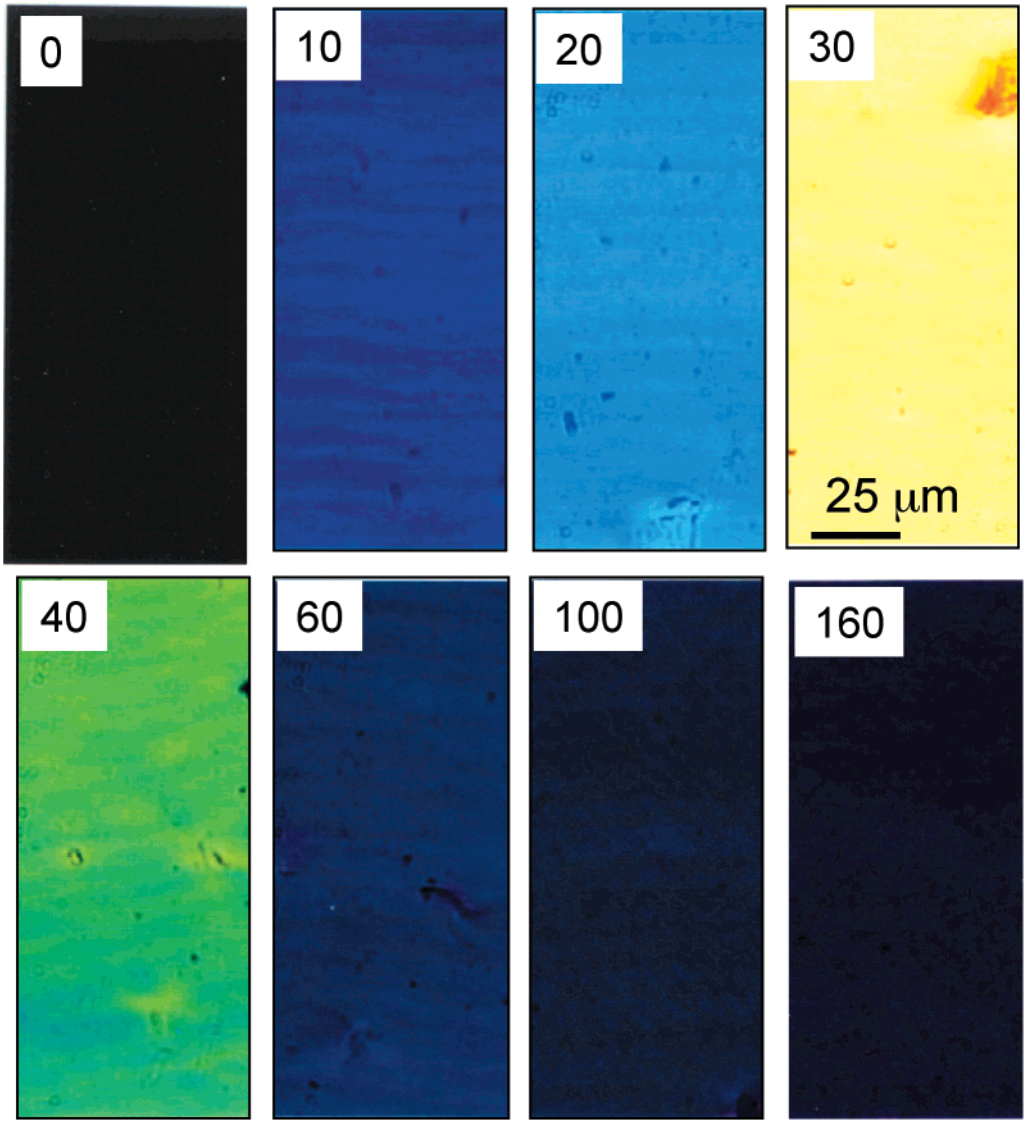

Figure 4. Sequence of in-situ polarizing optical microscopy (POM) micrographs during shear of PSHQ7 at $T = 177$ °C and using $\dot{\gamma} = 0.251$ s^{-1}. Flow is left-to-right and crossed polarizers are oriented with the polarizer along the flow axis. Sample thickness, $h = 50.8$ μm, and the plane being imaged contains the velocity and vorticity axes (1−3 plane). Times in seconds are shown with each image.

Upon cessation of flow (Figure 5, bottom row), the birefringent texture fades in a manner similar to PSHQ10, as reported previously[9] and for another system.[10] This relaxation to an isotropic, homogeneous state happens over a rapid time scale, but with rate depending on the duration of prior shearing.

Thus, we observe major differences, with in-situ POM flow experiments, between even-numbered and odd-numbered PSHQ*n* that should be interpreted in light of our measured odd−even terminal relaxation time data (see Table 1 and Figure 3). To enable such a quantitative correlation between orientation and rheological properties, we turn to spectrographic birefringence measurements.

Spectrographic Birefringence of Flow-Induced I−N Transition. Figure 6 shows a representative sequence of visible transmission spectra (without use of the multiorder $\lambda/2$ plate) during the shear of PSHQ7 at $T = 172$ °C ($\Delta T = 12$ °C) with $\dot{\gamma} = 1$ s^{-1}. Before shear (zero strain unit), the flat spectrum with $T(\lambda) = 100\%$ indicates an isotropic phase. Upon shear application, clear interference fringes appear with decreasing spectral spacing, indicative of increasing birefringence along the flow direction, to a steady value for accumulated shear strains $\dot{\gamma}t \geq 30$. On stopping flow, the spectra are observed to relax to the isotropic flat line over the course of 15 s, though complete relaxation follows exponential decay.

To extract birefringence reliably from visible transmission spectra using our described FFT method, even at low birefringence level near the threshold for nematic-phase formation, we have employed the multiorder retardation plate, as described in the Experimental Section, whose retardance is additive with that from flow-induced birefringence. Thus, it is easily accounted for using eq 1a. As a representative example, Figure 7 shows interference spectra for PSHQ10 at $T = 178$ °C ($\Delta T = 6$ °C) with the indicated $\dot{\gamma}$ increasing from bottom to top. Note that the spectra are all reported with the same scale factor and vertically shifted for clarity. To guide the eye, we have tracked one of the interference maxima with a thick dashed line. For low $\dot{\gamma}$, say $\dot{\gamma} < 0.5$ s^{-1}, flow does not alter the transmission spectrum. However, beyond a certain threshold value of $\dot{\gamma}$, in this

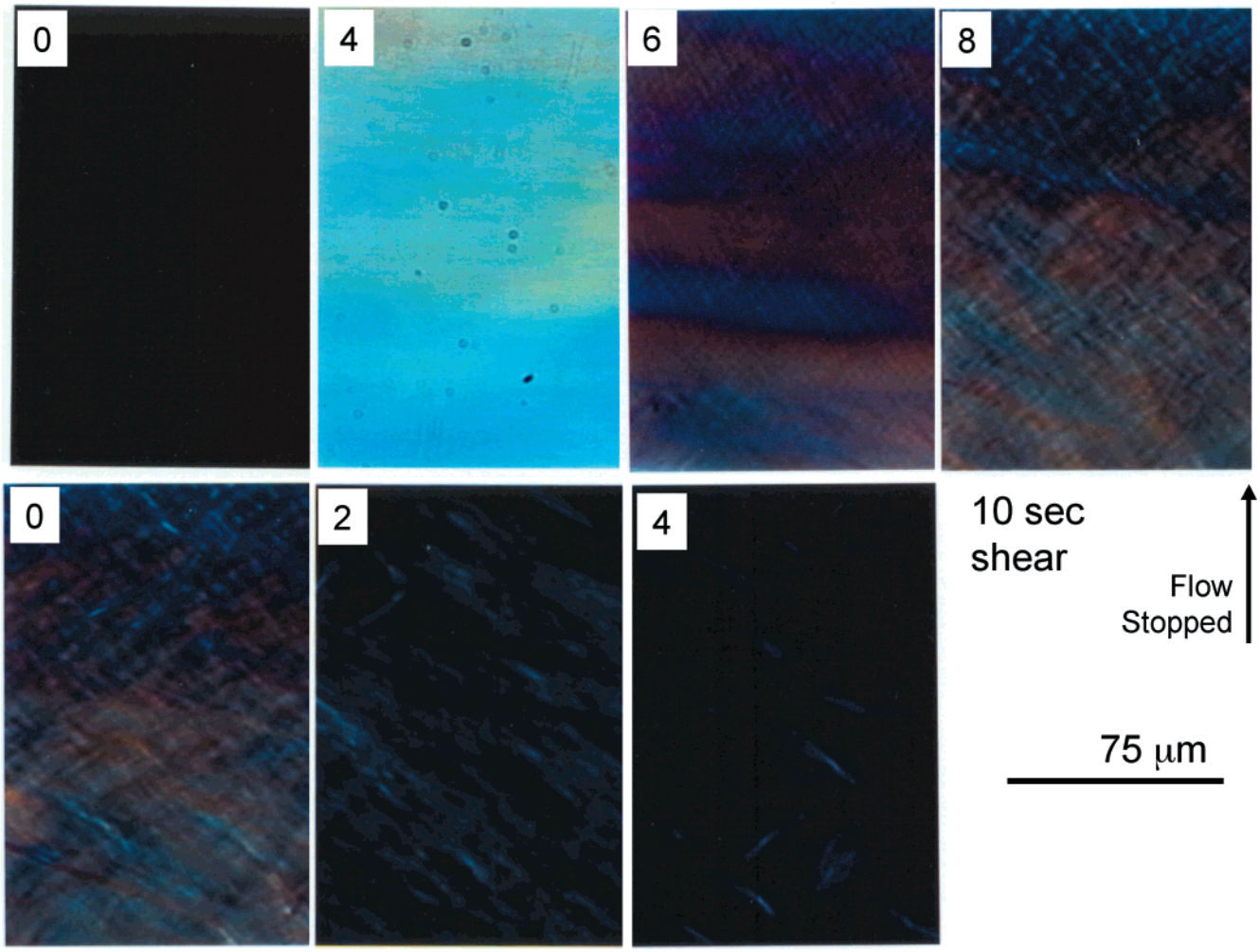

Figure 5. Sequence of in-situ POM images during shear start-up and relaxation for PSHQ6 at $T = 232$ °C, $\dot{\gamma} = 3.98$ s^{-1}, and $h = 50.8$ μm. Images on the top row were taken during shear at the times indicated in seconds, and shear was continued until 10 s. Images on the bottom row are following shear cessation with the times shown starting at the point of flow stoppage.

case $\dot{\gamma} = 0.398$ s^{-1}, the spectrum is altered due to sample birefringence, such that a given interference maximum (see the dashed line in Figure 7) shifts to lower wavelengths with increasing time (until steady state) and $\dot{\gamma}$ (until saturation). From Figure 7, it is clear that for PSHQ10 at $T = 178$ °C birefringence is continuing to increase—fringe spacing decreasing—even at $\dot{\gamma} = 10$ s^{-1}. Now, we analyze such spectra in light of eq 1a and using our FFT analysis method[8] to clearly observe trends in sample birefringence during flow-induced I−N transition.

Figure 8 shows an example of birefringence growth, $\Delta n^+(\dot{\gamma},t)$, under conditions favoring nematic conversion by shear. In this case, PSHQ7 is subjected to a shear flow of $\dot{\gamma} = 0.251$ s^{-1} at $T = 177$ °C, a temperature 9 °C above T^o_{IN}. We note that these are the same conditions used in generating the POM sequence of Figure 4. We see in this $\Delta n^+(\dot{\gamma},t)$ trace (and others) that an induction period of small birefringence exists, specifically the first 5 strain units, followed by a period of tremendous growth during the next 5 strain units (see also Figure 4, 30−40 s), leading to a maximum $\Delta n \cong 0.08$ at 55 s ($\dot{\gamma}t = 14$). This birefringence maximum yields to a drop toward a steady-state birefringence of $\Delta n \cong 0.067$ until flow cessation. On stopping flow, we observe exponential relaxation of sample birefringence toward zero with a single characteristic time (in this case) of $\tau = 16$ s. For all further discussions, we have examined the steady-state Δn (using $\dot{\gamma}t > 40$) as functions of spacer length, temperature, and shear rate.

To ascertain the critical conditions for flow-induced nematicity, we have measured steady-state birefringence of various PSHQ*n* as functions of both shear rate and temperature, as shown in Figure 9a−c for PSHQ6, PSHQ9, and PSHQ10, respectively. Flow birefringence values for temperatures well above T_{IN} for all samples are observed to be proportional to shear rate and to feature values $\Delta n < 0.001$, while flow birefringence in the nematic phase is weakly dependent on shear rate and in the range $0.1 < \Delta n < 0.2$.[16,18] We also note that the analogous traces for PSHQ8 (not presented here) are in qualitative agreement with PSHQ6 results, while the same agreement exists for PSHQ7 data (not presented here). In Figure 9a, we observe for PSHQ6 the existence of a temperature-dependent $\dot{\gamma}_{cr}$ beyond which birefringence grows in near proportion to $\dot{\gamma}$. At a constant Δn, the plots are shifted systematically to higher $\dot{\gamma}$ with increasing the temperature. Importantly, no plateau in Δn is observed for $\dot{\gamma} < 10$ s^{-1}, suggesting continued growth in the volume fraction of nematic phase (nematic fraction) at the $\dot{\gamma}$ we examined. Recall that Figure 5 showed evidence for significant nematic fibril formation in the same polymer sample under conditions captured by Figure 9a.

The results for PSHQ9, given in Figure 9b, show qualitatively similar results with important quantitative

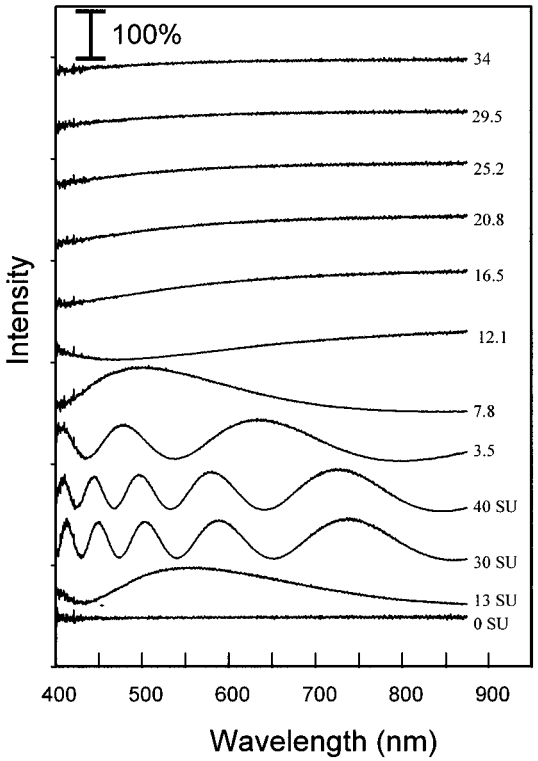

Figure 6. Visible transmission spectra using spectrographic birefringence optics (without the multiorder $\lambda/2$ plate of Figure 1) during shear start-up and relaxation of PSHQ7 at $T = 172$ °C and $\dot{\gamma} = 1$ s^{-1}. Reading from the bottom trace upward, shear is applied for 40 strain units and the spectra recorded during relaxation for the times indicated, referencing the time of cessation. All spectra feature the same scaling and are displaced vertically for clarity. Parallel polarizers are oriented 45° from the flow axis and sample thickness is 50.8 μm.

distinctions. In particular, it is observed that the $\dot{\gamma}_{cr}$ for onset of significant birefringence is much lower for comparable ΔT values. Thus, at higher $\dot{\gamma}$, continued growth in steady-state Δn toward a plateau value is expected to be only weakly dependent on temperature and indicative of pure nematic phase (full conversion). For $T = 168$ °C ($\Delta T = 8.6$ °C) the $\dot{\gamma}$ breadth from onset of nematic-phase nucleation to saturation is approximately 1.5 decades in shear rate. Results in nearly quantitative agreement have been observed for PSHQ7, another odd-numbered PSHQ*n*, but are not presented here due to space limitations.

The I−N transition behavior of PSHQ10 is very similar to that of PSHQ6, as shown in Figure 9c. Here, we observe dramatic onset of birefringence rise above a temperature-dependent $\dot{\gamma}_{cr}$, but with an absence of saturation for our limited $\dot{\gamma}$ range, as in the case of PSHQ6. These results are consistent with our previous results reported for PSHQ10,[9] where light transmitted between crossed polarizers was observed to increase dramatically above $\dot{\gamma} = 1.0$ s^{-1}. Importantly, however, we observe for PSHQ10 an intermediate plateau ($\Delta n \approx 0.005$) spanning a small range in $\dot{\gamma}$ (1 s^{-1} < $\dot{\gamma}$ < 5 s^{-1} for $T = 184$ °C). As this observation is made only for the PSHQ10 sample, the origin is unclear; however, we postulate that within the intermediate plateau the nematic phase formed consists primarily of high molecular weight species (with characteristically longer relaxation time), while the remaining fraction of molecular weight distribution undergoes conversion to nematic phase only at higher $\dot{\gamma}$. A nice test of this idea would be to examine the flow-induced transition for a binary mixture of near-monodisperse TLCPs with differing molecular weight.

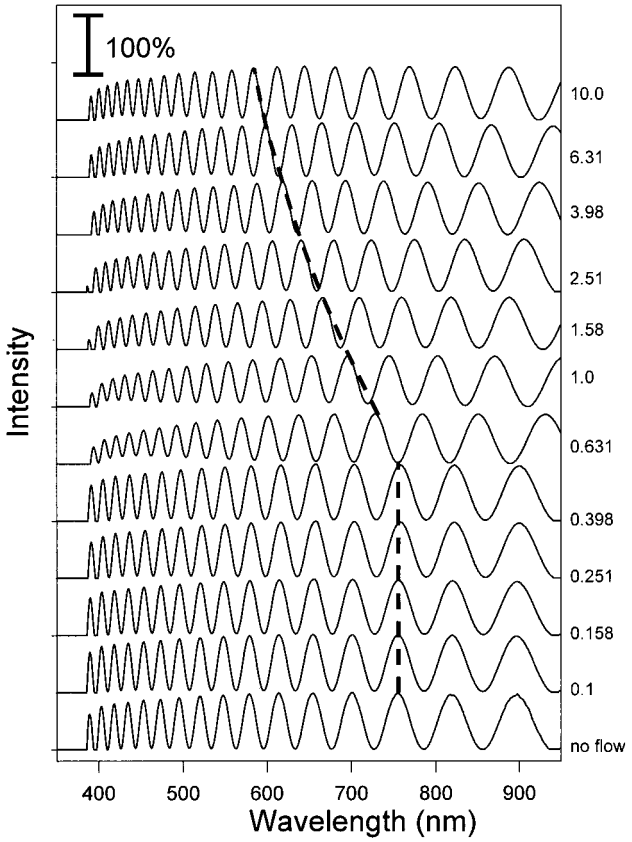

Figure 7. Visible transmission spectra using the setup shown schematically in Figure 1 (with the multiorder $\lambda/2$ plate) for PSHQ10 at the various shear rates indicated and for $T = 178$ °C. Scaling is held fixed and vertical displacement is used for clarity. A thick dashed line is drawn to aid the eye in following a particular spectral maximum with increasing shear rate (see text). Parallel polarizers are oriented 45° from the flow axis, the $\lambda/2$ plate is oriented with its slow axis parallel to flow, and sample thickness used is 50.8 μm.

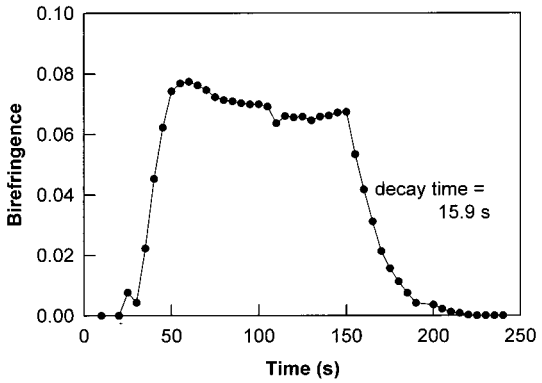

Figure 8. Example birefringence growth profile, $\Delta n + (\dot{\gamma},t)$, for PSHQ7 at $T = 177$ °C and $\dot{\gamma} = 0.251$ s^{-1}, as in Figure 4. Flow starts at $t = 0$ s and stops at $t = 150$ s ($\dot{\gamma}t = 37.5$).

Results for PSHQ8 (not presented here) are found to be similar to those of PSHQ6, but with a quantitative difference of higher $\dot{\gamma}_{cr}$ correlated with a lower intrinsic viscosity ([η] = 0.666 dL/g for PSHQ8 and [η] = 0.877 dL/g for PSHQ6),[13] and thus shorter relaxation time, for this polymer. In other words, the lower molecular weight of PSHQ8 compared to that of PSHQ6 was expected to yield a shorter terminal relaxation time and thus higher $\dot{\gamma}_{cr}$, and this is indeed borne out in our observations.

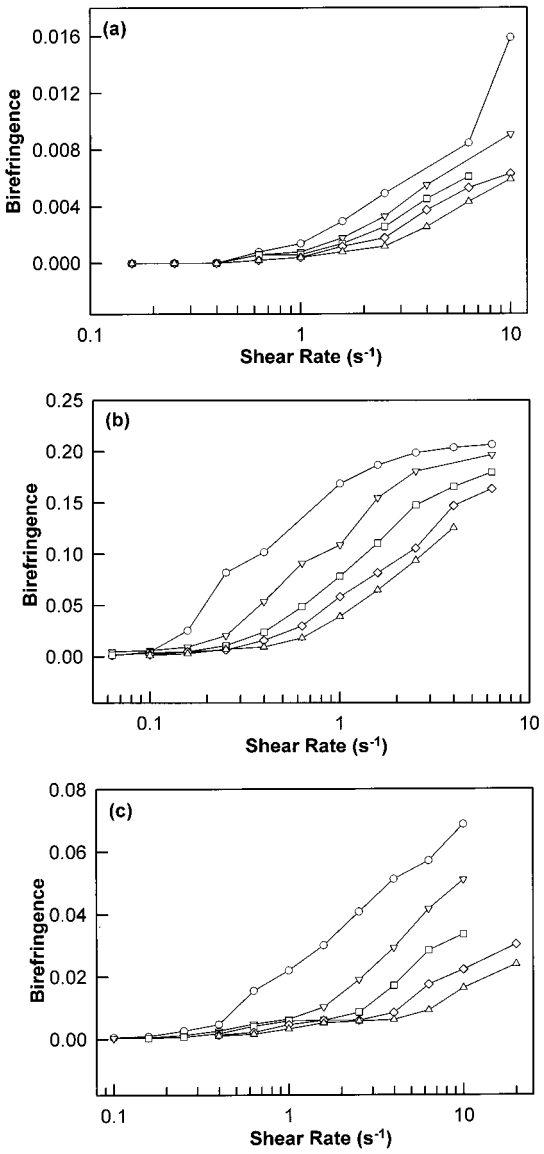

Figure 9. (a) Steady-state birefringence vs shear rate for PSHQ6 (T^{o}_{IN} = 220 °C) at various temperatures in the isotropic region: (○) 232, (▽) 234, (□) 236, (◇) 238, and (△) 240 °C. (b) Δn vs $\dot{\gamma}$ for PSHQ9 (T^{o}_{IN} = 159.4 °C) at various temperatures in the isotropic region: (○) 168, (▽) 170, (□) 172, (◇) 174, and (△) 176 °C. (c) Δn vs $\dot{\gamma}$ for PSHQ10 (T^{o}_{IN} = 171.8 °C) at various temperatures in the isotropic region: (○) 178, (▽) 180, (□) 182, (◇) 184, and (△) 186 °C.

Significant correlation between shear stress and birefringence measurements across the flow-induced transition exists in a manner similar to finding in side-chain LCPs,[10] but with important differences. Figure 10 shows a superposition of shear viscosity, shear stress, and birefringence plots as functions of $\dot{\gamma}$ for PSHQ9 at T = 170 °C (ΔT = 10.6 °C). For $\dot{\gamma} < 0.04$ s^{-1}, the polymer behaves mechanically as a Newtonian liquid and optically as an isotropic medium. For $\dot{\gamma} > 0.08$ s^{-1}, however, PSHQ9 begins to show optical evidence of nematic-phase formation. Above this plateau region (higher $\dot{\gamma}$) shear stress and birefringence climb dramatically, but to a limiting birefringence, Δn = 0.205 and to a peak in shear stress (measured torque) at $\dot{\gamma} \approx 0.5$ s^{-1}. During our rheological measurements we observed that for $\dot{\gamma} > 0.5$ s^{-1} the torque began to drop precipitously, suggesting an onset of flow instability. Therefore, in

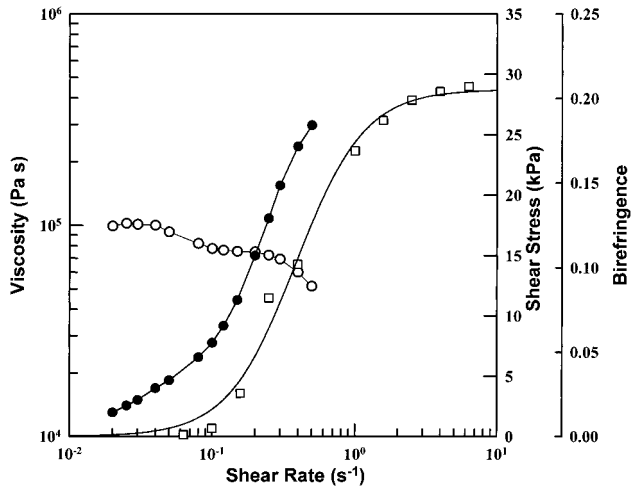

Figure 10. Superimposed shear stress (●), viscosity (○), and birefringence (□) vs shear rate plots for PSHQ9 at T = 170 °C, revealing a significant correlation between birefringence and shear stress (or viscosity) in the formation of a shear-induced nematic phase with increasing shear rate. See text for a detailed description.

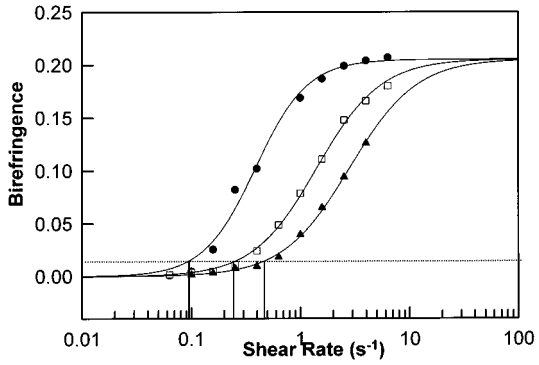

Figure 11. Fitting of $\Delta n - \dot{\gamma}$ data for PSHQ9 at 168 (●), 172 (□), and 176 °C (▲) using the logistics formula, eq 2.

Figure 10 we have not included viscosity or shear stress data for $\dot{\gamma} > 0.5$ s^{-1}.

Systematic quantification of the $\dot{\gamma}_{cr}$ for all samples and temperatures was facilitated through the use of the empirical relation of eq 2, where $\Delta n_{\infty}$is the plateau birefringence at full conversion, $\dot{\gamma}_0$ is an adjustable parameter corresponding to the midpoint in the rise of birefringence with $\dot{\gamma}$, and β is a parameter corresponding to the transition's $\dot{\gamma}$ breadth. We have found that β = 1.8 and Δn_{∞} = 0.20 yielded satisfactory fits to all data sets, allowing $\dot{\gamma}_0$ to remain as the sole adjustable parameter. Once $\dot{\gamma}_0$ was determined through nonlinear regression, eq 2 was solved to yield $\dot{\gamma}_{cr}$, where $\Delta n/\Delta n_{\infty}$ = 5%, i.e., to locate the $\dot{\gamma}_{cr}$ near the onset position. While the choice of 5% is arbitrary, this method was found to be robust through the use of all available data in the fitting procedure, rather than using only data near the transition onset. Figure 11 shows the quality of fitting observed for PSHQ9 along with the intersection of solid vertical lines with a dashed line at $\Delta n/\Delta n_{\infty}$ = 5% for determination of $\dot{\gamma}_{cr}$.

Following this analysis method for all PSHQ*n* samples and temperatures, we have plotted $\dot{\gamma}_{cr}$ as functions of ΔT, as shown in Figure 12. Immediately clear from this figure is a large breadth in $\dot{\gamma}_{cr}$ spanned by the PSHQ*n* polymers with varying spacer lengths. Indeed, this breadth appears to be comparable in magnitude with the terminal relaxation time data presented in Figure

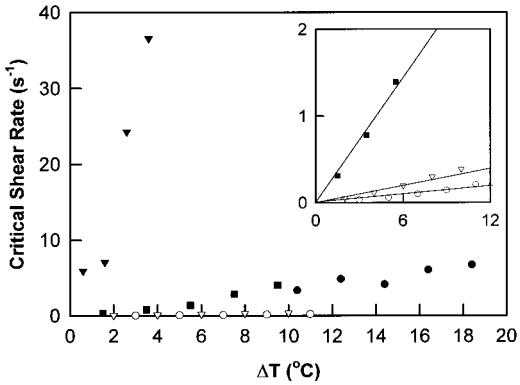

Figure 12. Plot of $\dot{\gamma}_{cr}$ vs ΔT (from curve fitting) for PSHQ6 (●), PSHQ7 (○), PSHQ8 (▼), PSHQ9 (▽), and PSHQ10 (■). The inset graph shows an expanded scale of the same axes.

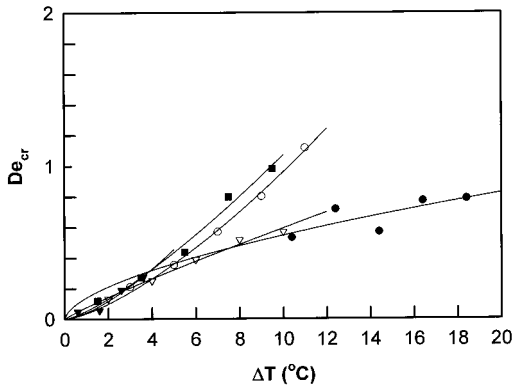

Figure 13. Critical Deborah number $De_{cr} = \dot{\gamma}_{cr}(T)\tau(T)$ vs ΔT for PSHQ6 (●), PSHQ7 (○), PSHQ8 (▼), PSHQ9 (▽), and PSHQ10 (■), revealing reasonable data collapse at low ΔT.

3, a point we turn to momentarily. It is observed, especially with the expanded inset plot of Figure 12, that PSHQ7 and PSHQ9 show similar behavior while PSHQ6 and PSHQ10 are equally grouped. PSHQ8, on the other hand, only allowed I−N transition for flows with high $\dot{\gamma}$ applied at temperatures close to T^{o}_{IN}. This is clearly correlated with the short relaxation times of this polymer reported in Figure 3.

Recognizing the inverse relationship between relaxation times, measured mechanically, and $\dot{\gamma}_{cr}$, measured rheo-optically, we have attempted to collapse the data plotted in Figure 12 by scaling the $\dot{\gamma}_{cr}(T)$ with the associated $\tau(T)$ values, thus defining a critical Deborah number, $De_{cr} = \dot{\gamma}_{cr}\tau$. The results of this scaling are presented in Figure 13 along with power-law fits of the form $De_{cr} = a(\Delta T)^b$ through each data set to guide the eye. We observe that this straightforward scaling approach works well for $\Delta T < 6$ °C but fails at higher values, perhaps due to oversimplification in our choice of the terminal relaxation time over other characteristic times. That good data collapse occurs for small ΔT suggests that nematic-phase formation is associated with a coupling between flow and the dynamics of large section of PSHQ*n* chains, not just the dynamics of mesogenic groups with presumed shorter relaxation time. This is apparent from the fact that we employed the terminal relaxation times for computing De_{cr}.

Concluding Remarks

We have observed a strong dependence of the flow-induced I−N transition phenomenon on the spacer length of the thermotropic polymers, PSHQ*n*. By combining optical and mechanical rheological observations of the transition, we have gained some insight into its origin, namely, the scaling of the I−N transition conditions with terminal relaxation time. We observe that as shear rate increases for a fixed temperature higher than the T^{o}_{IN}, a clear transition from low-level birefringence (0.0−0.005) to nematic-level birefringence (>0.01) is observed with comparatively high critical shear rates, $\dot{\gamma}_{cr}$, for even-numbered PSHQ*n* polymers than for odd-numbered PSHQ*n* polymers. This odd−even effect is explained by a significant difference in terminal relaxation times at fixed temperature above T^{o}_{IN}.[19]

Many details of the I−N transition phenomena remain unresolved, however, and demand further investigation. First, we have focused only on steady-state observations of the flow-induced transition, but we are certain that detailed *transient* studies of nematic-phase formation and relaxation to the isotropic phase will provide important elements to complete our picture of this nonequilibrium phase transition. Additionally, experiments that decompose the orientational order into that of the mesogen and of the spacer are needed. Such data, if available through the I−N transition, will allow discernment of the sequence of events that occur on going from an isotropic to nematic phase. Specifically, we would like to differentiate two possibilities: (1) PSHQ*n* chains first extend in flow and then (on continued shearing) spontaneously align in nematic domains, and (2) nematic domains nucleate from PSHQ*n* chains with only local ordering and numerous hairpins, following which chain extension continues to completion. By better understanding the details of this process at the molecular level, we hope that a quantitative model will be enabled with predictive capability for more complex flow geometries of relevance to industrial processes such as fiber spinning and injection molding.

Acknowledgment. P.T.M. acknowledges partial financial support of this research by the Air Force Office of Scientific Research under Grant F49620-00-1-0100 and the National Science Foundation under Grant CTS-0093880 and fruitful discussions with P. Olmsted. C.H.D. acknowledges the support of this research by the National Science Foundation under Grant CTS-9614929.

References and Notes

(1) Kim, S. S.; Han, C. D. *Macromolecules* **1993**, *26*, 3176.
(2) Kim, S. S.; Han, C. D. *J. Polym. Sci., Part B: Polym. Phys.* **1994**, *32*, 371.
(3) Han, C. D.; Chang, S.; Kim, S. S. *Macromolecules* **1994**, *27*, 7699 and references therein.
(4) Kim, S. S.; Han, C. D. *J. Rheol.* **1993**, *37*, 847.
(5) Kim, S. S.; Han, C. D. *Macromolecules* **1993**, *26*, 6633.
(6) Han, C. D.; Kim, S. S. *J. Rheol.* **1994**, *38*, 13.
(7) Chang, S.; Han, C. D. *Macromolecules* **1997**, *30*, 2021.
(8) Mather, P. T.; Jeon, H. G.; Han, C. D.; Chang, S. *Macromolecules* **2000**, *33*, 7594.
(9) Mather, P. T.; Romo-Uribe, A.; Han, C. D.; Kim, S. S. *Macromolecules* **1997**, *30*, 7977.
(10) Pujolle-Robic, C.; Noirez, L. *Nature (London)* **2001**, *409*, 167.
(11) Olmsted, P.; Lu, C. Y. D. *Phys. Rev. E* **1999**, *60*, 4397.
(12) Berret, J. F.; Roux, D. C.; Porte, G.; Lindler, P. *Europhys. Lett.* **1994**, *25*, 521.
(13) Chang, S.; Han, C. D. *Macromolecules* **1997**, *30*, 1670.
(14) Furukawa, A.; Lenz, R. W. *Macromol. Chem. Macromol. Symp.* **1986**, *2*, 3.
(15) Kim., S. S.; Han, C. D. *Polymer* **1994**, *35*, 93.
(16) Kim, D.-O.; Han, C. D.; Mather, P. T. *Macromolecules* **2000**, *33*, 7922.
(17) Mather, P. T.; Stuber, H.-R.; Chaffee, K. P.; Haddad, T. S.; Romo-Uribe, A.; Lichtenhan, J. D. *MRS Symp. Proc.* **1996**, *425*, 137.

(18) Han, C. D.; Chang, S.; Mather, P. T.; Fang, X. *Macromolecules* **2001**, *34*, 7152.

(19) As the present study deals with flow-induced phase transition from the isotropic phase, we have used the terminal relaxation times determined in the isotropic region in computing $De_{crit.}$

MA0115601